SRSF1-mediated alternative splicing of *Tial1*/*Tiar* is essential for homing and self-renewal in mouse spermatogonial stem cells

Longjie Sun[1], Zheng Lv[1], Xuexue Chen[1], Rong Ye[4], Shuang Tian[1], Chaofan Wang[1], Xiaomei Xie[1], Lu Yan[1], Xiaohong Yao[1], Yujing Shao[1], Sheng Cui[3], Juan Chen[2, *], and Jiali Liu[1, *]

[1]State Key Laboratory of Animal Biotech Breeding, College of Biological Sciences, China Agricultural University, Beijing, 100193, China.

[2]Key Laboratory of Precision Nutrition and Food Quality, Department of Nutrition and Health, China Agricultural University, Beijing, 100190, China.

[3]College of Veterinary Medicine, Yangzhou University, Yangzhou, Jiangsu, 225009, China.

[4]Key Laboratory of RNA Biology, Institute of Biophysics, Chinese Academy of Sciences, Beijing, 100101, China.

*Correspondence: chenjuan.09@163.com (J.C.), liujiali@cau.edu.cn (J.L.)

Abstract

Spermatogonial stem cells (SSCs) are essential for continuous spermatogenesis and male fertility. The underlying mechanisms of alternative splicing (AS) in mouse SSCs are still largely unclear. We demonstrated that SRSF1 is essential for gene expression and splicing in mouse SSCs. Crosslinking immunoprecipitation and sequencing (CLIP-seq) data revealed that spermatogonia-related genes (e.g., *Plzf*, *Id4*, *Setdb1, Stra8*, *Tial1*/*Tiar*, *Bcas2*, *Ddx5*, *Srsf10*, *Uhrf1*, and *Bud31*) were bound by SRSF1 in the mouse testes. Specific deletion of *Srsf1* in mouse germ cells impairs homing and self-renewal of SSCs leading to male infertility. Whole-mount staining data showed the absence of germ cells in the testes of adult cKO mice, which indicates Sertoli cell-only syndrome (SCOS) in cKO mice. The expression of spermatogonia-related genes (*Gfra1*, *Pou5f1*, *Plzf*, *Dnd1*, *Stra8*, and *Taf4b*) was significantly reduced in the testes of conditional knockout (cKO) mice. Moreover, multiomics analysis suggests that SRSF1 directly binds and regulates the expression of *Tial1*/*Tiar* via AS to implement SSC homing and self-renewal. In addition, immunoprecipitation mass spectrometry (IP-MS) data showed that SRSF1 interacts with RNA splicing-related proteins (e.g., SRSF10, SART1, RBM15, SRRM2, SF3B6, and SF3A2). Collectively, our data reveal the critical role of SRSF1-mediated AS in SSC homing and self-renewal, which may provide a framework to elucidate the molecular mechanisms of the posttranscriptional network underlying the formation of SSC pools and the establishment of niches.

Keywords

SRSF1, alternative splicing, infertility, Sertoli cell-only syndrome, spermatogonial stem cells, homing, self-renewal

Introduction

SCOS, also known as del Castillo syndrome or germ cell aplasia, is one of the most common causes of severe non-obstructive azoospermia (NOA) (Wang et al., 2023). SCOS is the presence of only Sertoli cells in the testicular tubules of the testes, with no germ cells present (Juul et al., 2014; Wang *et al.*, 2023). It is well known that abnormal self-renewal and differentiation of SSCs leads to SCOS (Kanatsu-Shinohara and Shinohara, 2013; La and Hobbs, 2019b). Gonocyte begin homing at 0 to 3 days postpartum (dpp) and then develop into SSCs at 4 to 6 dpp for continuous self-renewal and differentiation (Lee and Shinohara, 2011; McLean et al., 2003; Tan and Wilkinson, 2020). The mechanisms regulating spermatogonia homing are hence crucial for forming SSC pools and establishing niches (Oatley and Brinster, 2012). Spermatogonia migrate to form two distinct subtypes in mice. The first subtype develops into an SSC population that provides progenitor spermatogonia for adult spermatogenesis, whereas the second subtype transitions directly to differentiated spermatogonia that contribute to the first round of spermatogenesis but do not self-renew (Kluin and de Rooij, 1981; Law et al., 2019). Therefore, SSC homing to establish niches is essential for SSC self-renewal and differentiation.

Many transcription factors (e.g., FOXO1, PLZF, POU5F1, TAF4B, CHD4, BCL6B, BRACHYURY, ETV5, ID4, LHX1, POU3F1, DMRT1, NGN3, SOHLH1, SOHLH2, SOX3, and STAT3) promote SSC self-renewal and differentiation (Cafe et al., 2021; Song and Wilkinson, 2014). However, the molecular mechanisms of the posttranscriptional network underlying SSC homing and self-renewal are not sufficiently clear. Previous studies have identified the key RNA-binding proteins DND1 and DDX5 in SSCs with a unique and dominant role in posttranscriptional regulation (Legrand et al., 2019; Yamaji et al., 2017). Surprisingly, recent studies have found that the RNA-binding proteins SRSF10, UHRF1, BUD31, and BCAS2 regulate AS in mouse spermatogonia (Liu et al., 2022; Liu et al., 2017; Qin et al., 2023; Zhou et al., 2022). It is well known that testes are rich in AS events (Mazin et al., 2021; Venables, 2002). Thus, understanding the mechanisms of AS in human reproduction can provide new insights into clinical diagnosis. However, the underlying mechanisms of how AS functions in SSC homing and self-renewal are still largely unclear.

Serine/arginine-rich splicing factor 1 (SRSF1; previously SF2/ASF) is a widely studied and important splicing factor involved in cancer progression, heart development, and thymus development (Du et al., 2021; Katsuyama et al., 2019; Katsuyama and Moulton, 2021; Liu et al., 2021; Lv et al., 2021; Qi et al., 2021; Xu et al., 2005). Our previous work has shown that SRSF1 deficiency impairs primordial follicle

formation during meiotic prophase I and leads to primary ovarian insufficiency (POI) (Sun et al., 2023). However, the underlying mechanisms by which SRSF1 regulates pre-mRNA splicing in mouse SSCs remain unknown. A mouse model with *Srsf1* conditional deletion can effectively address this uncertainty. This study showed that specific deletion of *Srsf1* in mouse germ cells leads to NOA by impairing homing and self-renewal in mouse SSCs. We further verified that SRSF1 directly binds and regulates *Tial1*/*Tiar* expression via AS, which is critical for homing and self-renewal in mouse SSCs.

Results

SRSF1 has an essential role in mouse testes

To investigate the role of SRSF1 in spermatogenesis, the dynamic localization of SRSF1 in the testis was evaluated. Fascinatingly, the results of SRSF1 and γH2AX co-staining revealed that SRSF1 was expressed in spermatogenesis (Figure 1A and S1). RT–qPCR and Western blotting results showed that the expression of SRSF1 fluctuated during the developmental stages of the testes (Figure 1B and 1C). Concurrently, the results of SRSF1 and PLZF co-staining revealed that SRSF1 was highly expressed in the nuclei of spermatogonia (Figure 1D). To further explore the function of SRSF1 in regulating SSC self-renewal and differentiation, CLIP-seq was performed in adult mouse testes. GO enrichment analyses of the SRSF1 peak-containing genes revealed that spermatogenesis-related genes were regulated by SRSF1 (Figure 2A and Table S1). In combination with previous studies, we found that spermatogonia-related genes (*Plzf*, *Id4*, *Setdb1, Stra8*, *Tial1*/*Tiar*, *Bcas2*, *Ddx5*, *Srsf10*, *Uhrf1*, and *Bud31*) were bound by SRSF1. To provide in-depth insight into the binding of spermatogonia-associated genes, the SRSF1-binding peaks of the gene transcripts were shown by using IGV (Figure 2B). The co-staining results showed localization and expression of the spermatogonia-related protein in mouse testes (Figure 2C). SRSF1 has a vital role in posttranscriptional regulation in the testes, particularly during SSC self-renewal and differentiation.

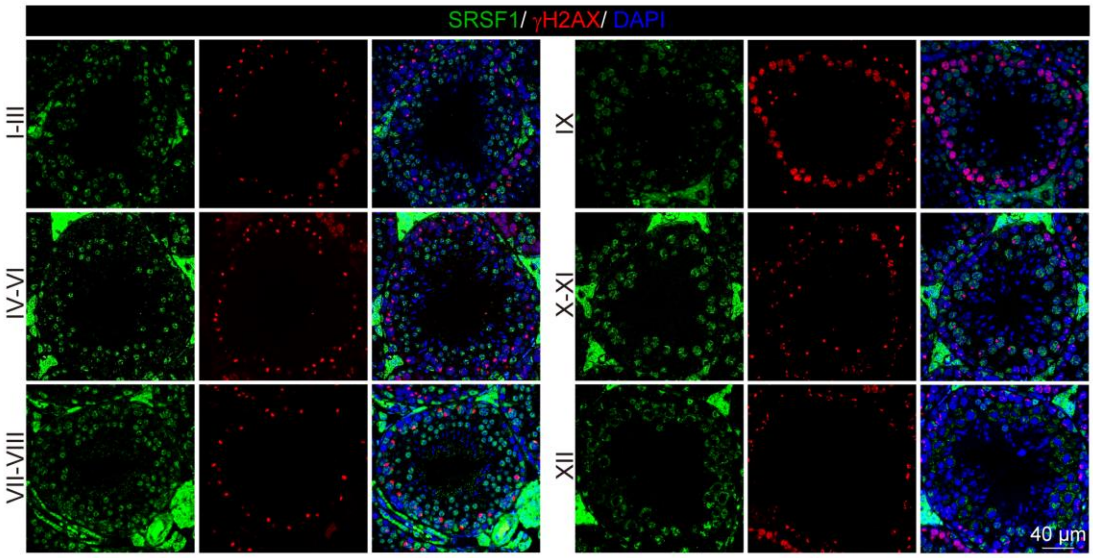

Figure S1. Dynamic localization of SRSF1 during spermatogenesis.

Co-immunostaining was performed using SRSF1 and γH2AX antibodies from adult mouse testes. DNA was stained with DAPI. Scale bar, 40 μm.

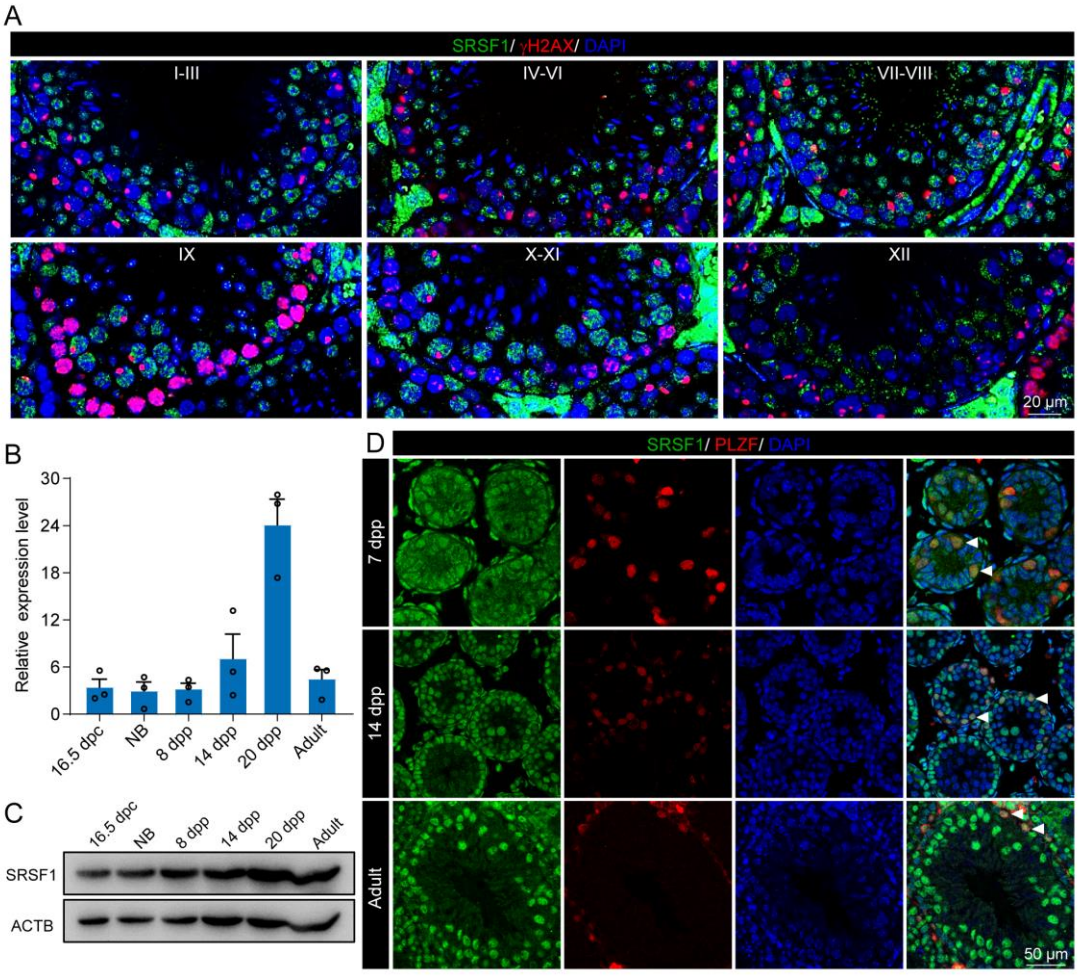

Figure 1 Dynamic localization of SRSF1 in male mouse germ cells.

(A) Dynamic localization of SRSF1 during spermatogenesis. Co-immunostaining was performed using SRSF1 and γH2AX antibodies from adult mouse testes. DNA was stained with DAPI. Scale bar, 20 μm.

(B) Expression of *Srsf1* in testes at different stages of development. The RT–qPCR data were normalized to *Gapdh*. *n*=3.

(C) Western blotting of SRSF1 expression in testes at different stages of development. GAPDH served as a loading control.

(D) Localization and expression of SRSF1 in spermatogonia. Co-immunostaining was performed using PLZF and SRSF1 antibodies from 7 dpp, 14 dpp, and adult mouse testes. DNA was stained with DAPI. Arrowheads, spermatogonia. Scale bar, 50 μm.

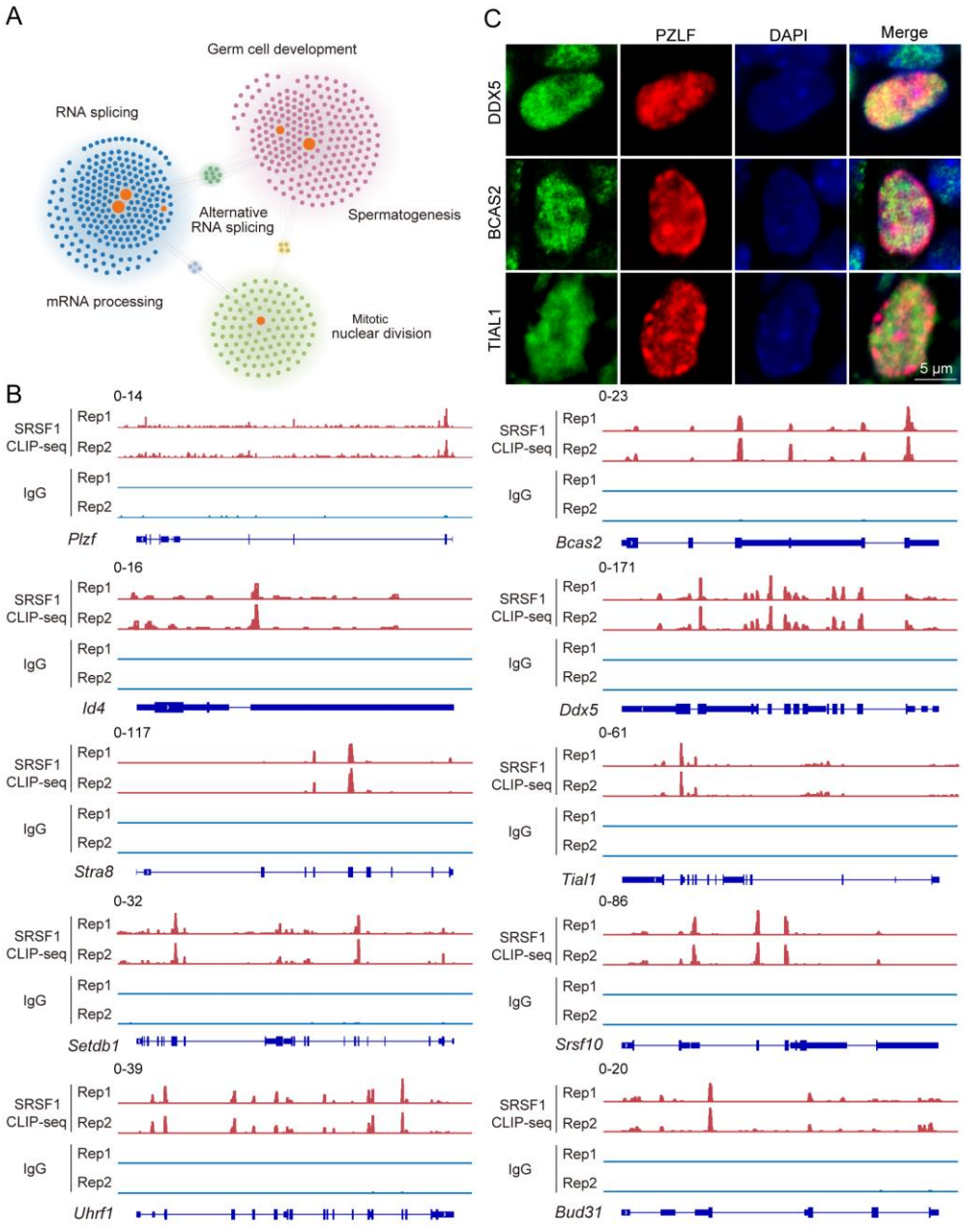

Figure 2 SRSF1-binding genes have an essential role in SSC self-renewal and differentiation.

(A) Network showing GO enrichment analyses of SRSF1-binding genes.

(B) Representative genome browser views of spermatogonia-related gene transcripts bound by SRSF1.

(C) Localization and expression of the spermatogonia-related protein in mouse testes. Scale bar, 5 μm.

SRSF1 deficiency leads to SCOS

To define the specific involvement of SRSF1 in SSC self-renewal and differentiation, we studied the physiological roles of SRSF1 in vivo using a mouse model. Considering that global SRSF1 knockout is lethal in mice (Xu *et al.*, 2005), we used a conditional allele of *Srsf1* (*Srsf1*^{Fl}) in which exons 2, 3, and 4 of *Srsf1* are flanked by two *loxP* sites (Figure 3A). By crossing *Srsf1*^{Fl} and *Vasa*-Cre mice, we obtained *Vasa*-Cre *Srsf1*$^{Fl/Fl}$ mice with *Srsf1* deletion in germ cells (Figure 3A and 3B). We verified the absence of the SRSF1 protein in germ cells by co-immunofluorescence analyses with SRSF1 and PLZF antibodies (Figure 3C). Subsequently, the breeding experiment indicated that cKO mice had a standard mating capacity but that the absence of *Srsf1* led to complete infertility in cKO males (Figure 3D). Histological examination of cKO epididymides revealed that sperm could not be found in the cauda epididymis (Figure 3E). Considering the limitations of sectioning, the cauda epididymal sperm count further validated this conclusion (Figure 3F). It was clear that spermatogenesis in the testes was severely impaired. Therefore, we focused our attention on the testes. The adult cKO mice were normal in size (Figure 3G). However, the sizes of cKO mouse testes were significantly reduced (Figure 3H). Histological examination of cKO testis sections showed that no germ cells could be visualized, and only a large number of Sertoli cells were observed in the testes of cKO mice (Figure 3I). Together, these results demonstrated that SRSF1 is critical for spermatogenesis and that its absence leads to SCOS.

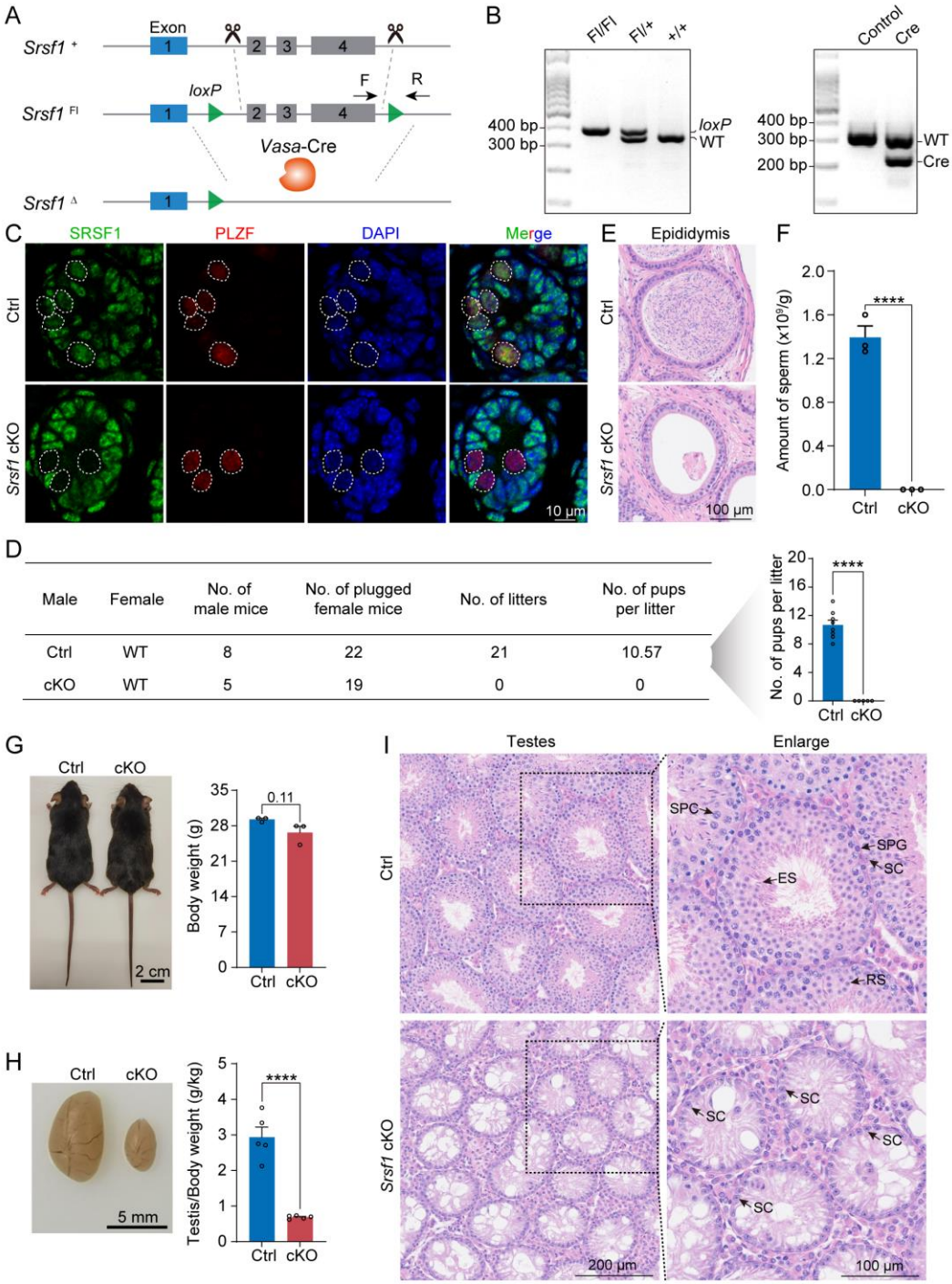

Figure 3 SRSF1 plays critical roles in spermatogenesis and male fertility.

(A) *Vasa*-Cre mice were crossed with *Srsf1*$^{Fl/Fl}$ mice to generate *Srsf1* cKO mice. Cre-mediated deletion removed exons 2, 3, and 4 of *Srsf1* and generated a null protein allele.

(B) Genotyping PCR was performed using *Vasa*-Cre and *Srsf1* primers.

(C) Co-immunostaining of SRSF1 and PLZF in 7 dpp Ctrl and cKO testes. DNA was stained with DAPI. Scale bar, 10 μm.

(D) Fertility test results showed a male infertility phenotype in the cKO mice (n= 5) compared to the Ctrl mice (n= 8).

The number of pups per litter was determined in the cKO (n= 5) and Ctrl (n= 8) mice.

(E) Haematoxylin-eosin-stained epididymis sections from adult Ctrl and cKO mice were obtained. Scale bar, 100 μm.

(F) Cauda epididymal sperm counting was performed. n=3.

(G) Normal body weight in cKO mice. The body sizes and weights of adult Ctrl and cKO mice are shown as the mean ± SEM. n= 3.

(H) Testis atrophy in adult cKO mice. Testis sizes and weights of adult Ctrl and cKO mice are shown as the mean ± SEM. n= 5.

(I) Haematoxylin-eosin-stained testis sections from adult Ctrl and cKO mice were obtained. Scale bar, left panel: 200 μm, right panel: 100 μm. SC, Sertoli cell; SPG, spermatogonia; SPC, spermatocyte; RS, round spermatid; ES, elongated spermatid.

Unpaired Student's t test determined significance; exact P value $P \geq 0.05$, ****$P < 0.0001$. The points and error bars represent the mean ± SEM.

Loss of SRSF1 impairs SSC homing and self-renewal

To further confirm the absence of germ cells in the testes of cKO mice, PLZF and γH2AX co-staining was performed in adult mouse testes. These data suggested that SRSF1 deficiency impaired germ cell survival (Figure 4A). The results of VASA and TRA98 co-staining further confirmed this phenotype (Figure 4B). Considering the limitations of sectioning, we used whole-mount immunostaining to perform a comprehensive analysis and found that germ cells were indeed absent in the testes of cKO mice (Figure 4C). To dynamically analyse the loss of germ cells, we collected testes from 5 dpp, 7 dpp, and 14 dpp mice. Morphological results showed that the testes of 7 dpp and 14 dpp cKO mice were much smaller than those of Ctrl mice (Figure 5A). To determine the presence of germ cells in cKO testes, VASA staining was performed in 5 dpp, 7 dpp, and 14 dpp Ctrl and cKO testes. The results showed that germ cells were still present in cKO mice but were significantly reduced in 7 dpp and 14 dpp cKO testes (Figure 5B). The germ cell count per tube showed a significant reduction in the number of 7 dpp and 14 dpp cKO testes, especially 14 dpp cKO testes (Figure 5C). In addition, TUNEL results showed that apoptosis significantly increased in cKO testes (Figure 5D). These data suggested that the absence of SRSF1 causes apoptosis in a large number of spermatogonia that are unable to self-renew. Interestingly, the results of VASA and SOX9 co-staining showed that partial germ cells could not complete homing in 5 dpp cKO testes (Figure 5E). Thus, all the above data indicated that SRSF1 has an essential role in the

192 homing and self-renewal of spermatogonia.

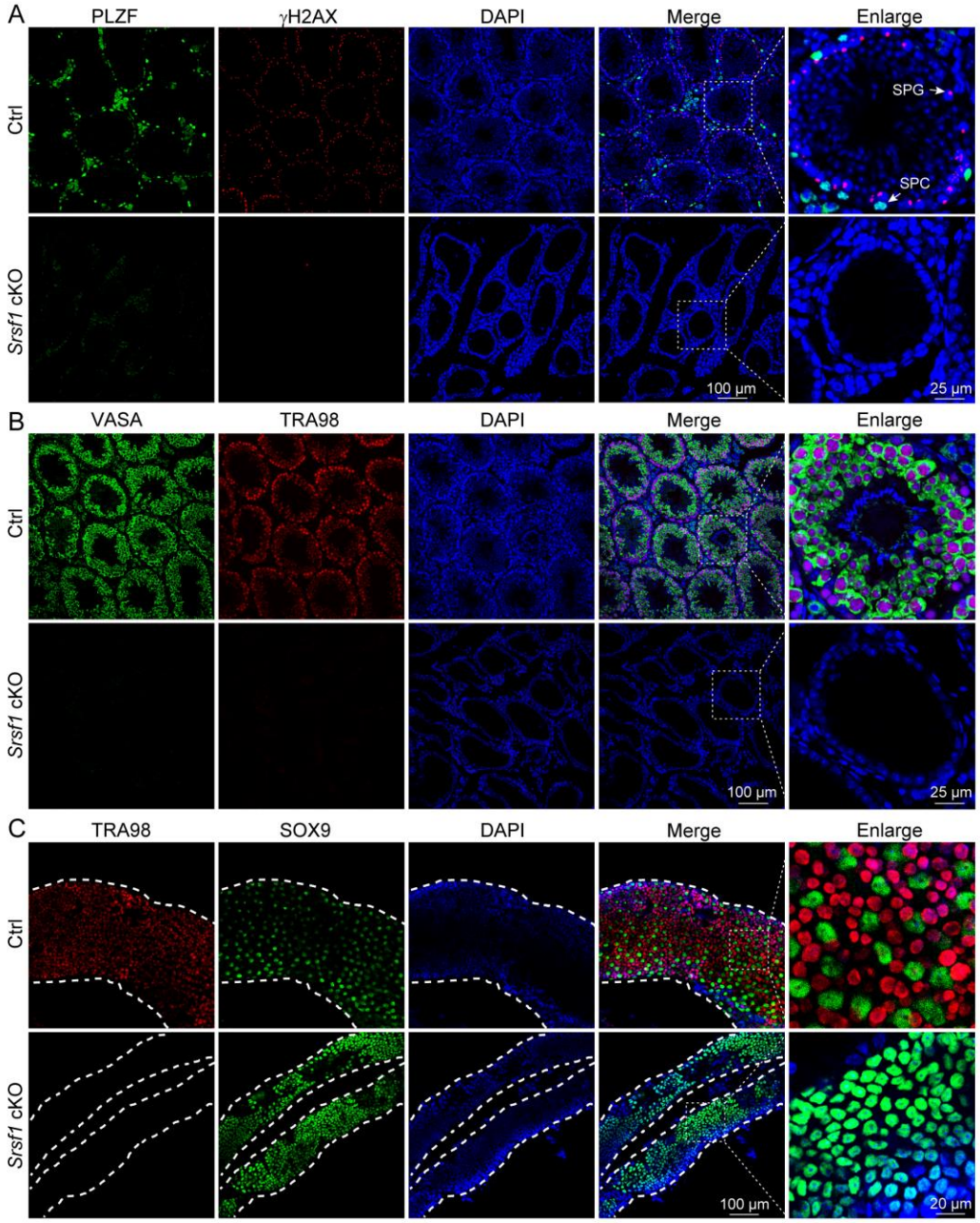

193

194 **Figure 4 Loss of germ cells in adult cKO mouse testes.**

195 (A) Co-immunostaining of PLZF and γH2AX in adult Ctrl and cKO testes. DNA was stained with DAPI. Scale bar,

196 right panel: 25 μm, other panels: 100 μm.

197 (B) Co-immunostaining of VASA and TRA98 in adult Ctrl and cKO testes. DNA was stained with DAPI. Scale bar,

198 right panel: 25 μm, other panels: 100 μm.

199 (C) Whole-mount co-immunostaining of TRA98 and SOX9 in adult Ctrl and cKO testes. DNA was stained with

200 DAPI. White dashed lines, boundary of the tubule. Scale bar, right panel: 20 μm, other panels: 100 μm.

201

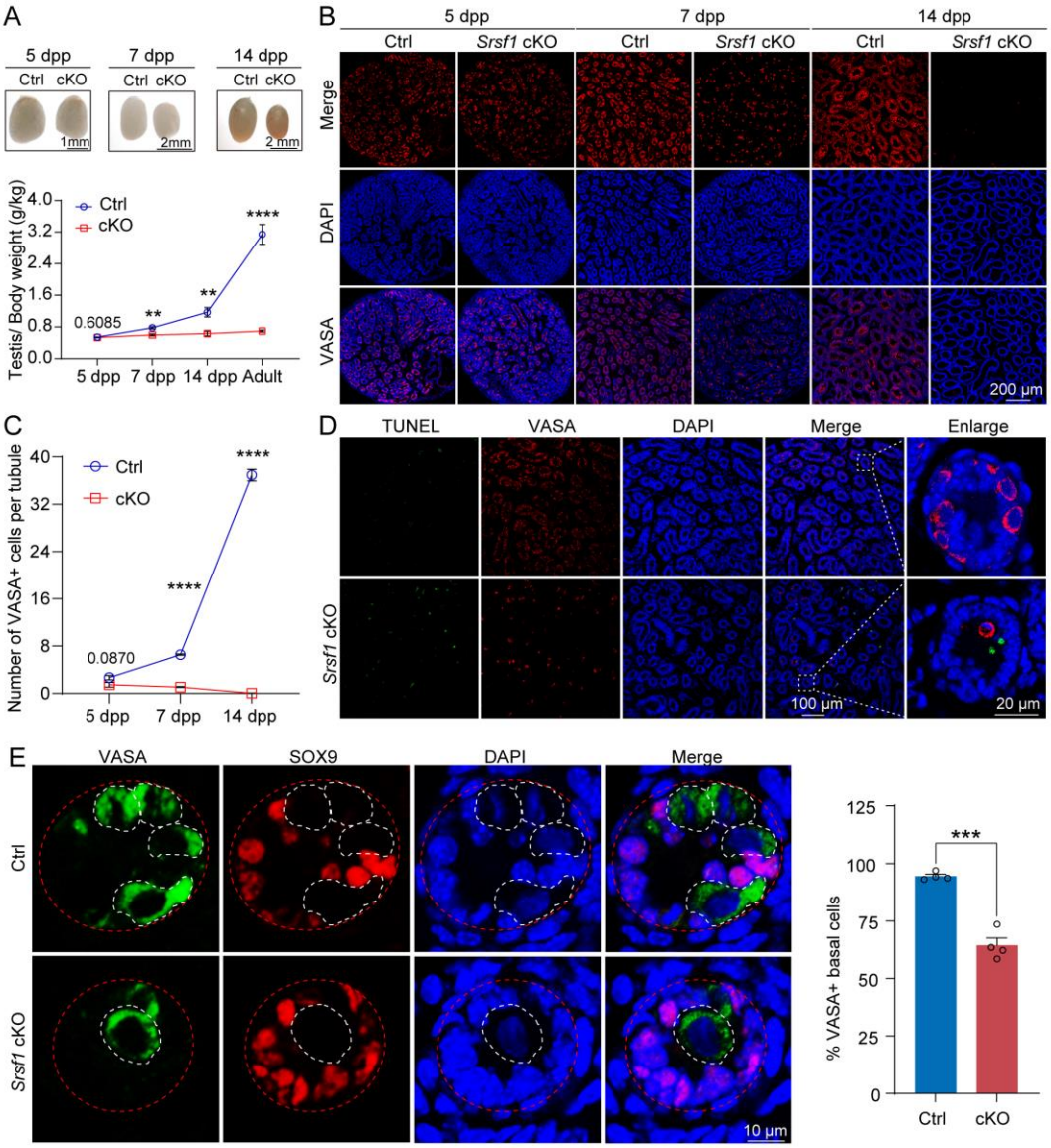

Figure 5 SRSF1 is required for SSC homing and self-renewal.

(A) Testis sizes of 5 dpp, 7 dpp, and 14 dpp Ctrl and cKO mice are shown. The testis/body weight ratios (g/kg) of 5 dpp, 7 dpp, 14 dpp, and adult Ctrl and cKO mice are shown as the mean ± SEM. n= 4.

(B) Immunostaining of VASA in 5 dpp, 7 dpp, and 14 dpp Ctrl and cKO testes. DNA was stained with DAPI. Scale bar, 200 μm.

(C) Number of VASA-positive cells per tubule is the mean ± SEM. n= 3.

(D) TUNEL apoptosis assay was performed on sections from 7 dpp Ctrl and cKO testes. DNA was stained with DAPI. Scale bar, right panel: 20 μm, other panels: 100 μm.

(E) Co-immunostaining of VASA and SOX9 in 5 dpp Ctrl and cKO testes. DNA was stained with DAPI. Scale bar, 10 μm. Red dashed circles, tubule. White dashed circles, germ cell. the percentage of VASA positive basal cells is shown as the mean ± SEM. n= 4.

Unpaired Student's *t* test determined significance; exact *P* value $P \geq 0.05$, $^{**}P < 0.01$, $^{***}P < 0.001$, $^{****}P < 0.0001$. The points and error bars represent the mean ± SEM.

SRSF1 is essential for gene expression in SSC homing and self-renewal

To investigate the molecular mechanisms of SRSF1 in SSC homing and self-renewal, we isolated mRNA from 5 dpp cKO and Ctrl mouse testes and performed RNA-seq. RNA-seq and RT–qPCR results showed a significant reduction in the expression of SRSF1 in 5 dpp cKO mouse testes (Figure 6A). Western blotting results showed that SRSF1 expression was significantly reduced in the testes of cKO mice at 5 dpp (Figure 6B). Hence, for Ctrl and cKO samples, the confidence level of the RNA-seq data was high. The volcano map and cluster heatmap showed 715 downregulated and 258 upregulated genes identified by RNA-seq data in 5 dpp cKO mouse testes (Figure 6C, 6D and Table S2). These gene GO enrichment analyses indicated abnormal germ cell development and cell cycle arrest in 5 dpp cKO mouse testes (Figure 6E). Surprisingly, the heatmap showed that SSC homing and self-renewal-associated gene (*Gfra1*, *Pou5f1*, *Plzf*, *Nanos3*, *Dnd1*, *Stra8*, and *Taf4b*) expression was significantly reduced in the testes of cKO mice at 5 dpp (Figure 6F). Simultaneously, visual analysis using IGV showed that the peak of SSC-related genes was significantly decreased (Figure 6G). Next, we validated the abnormal expression of SSC homing and self-renewal associated genes (downregulated: *Gfra1*, *Pou5f1*, *Plzf*, *Dnd1*, *Stra8*, and *Taf4b*; stabilized: *Nanos3*) by RT–qPCR (Figure 6H). Together, these data indicated that germ cell-specific deletion of SRSF1 impairs the expression of SSC-related genes.

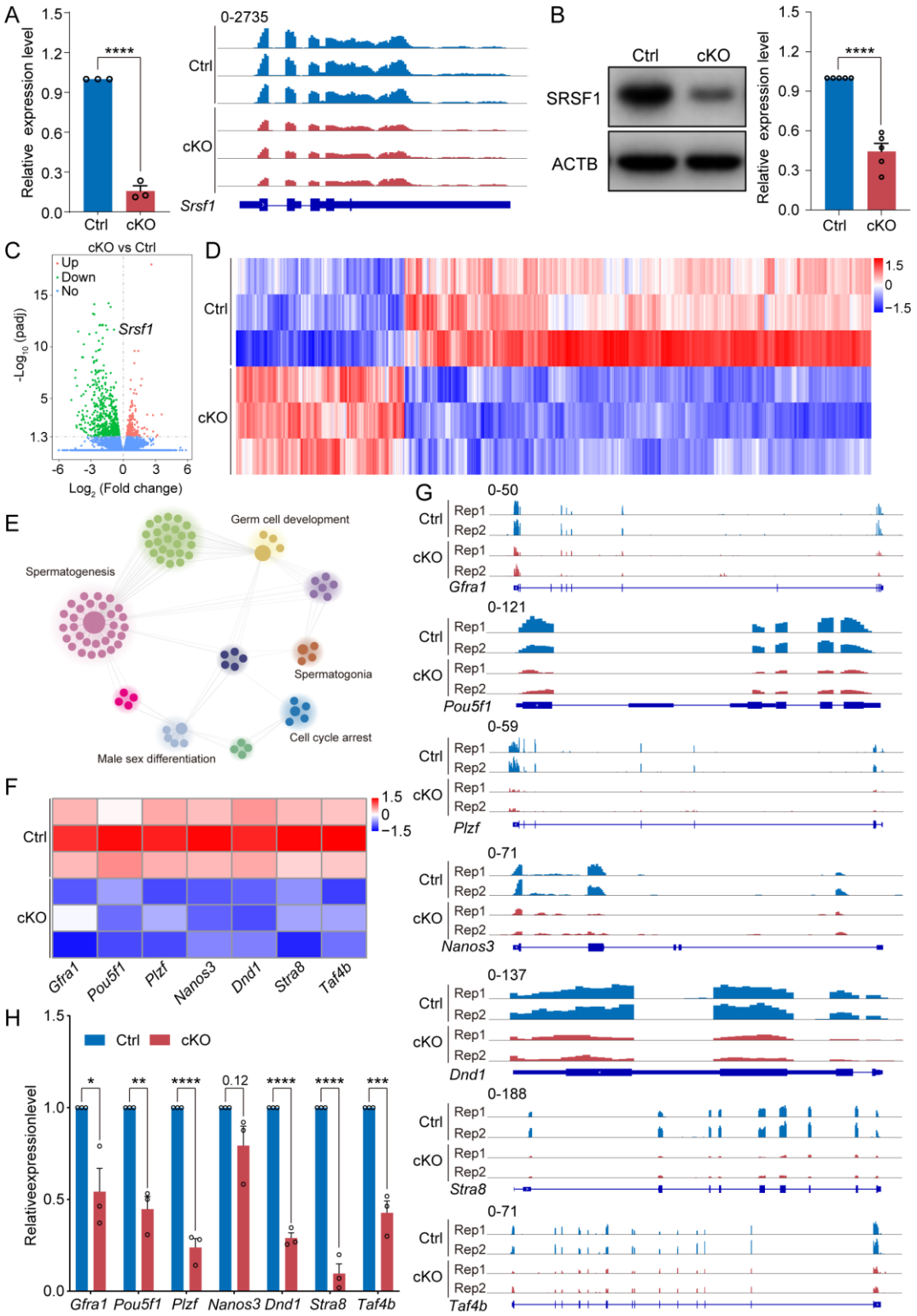

234

235 **Figure 6 SRSF1 regulates the expression of critical genes in the homing and self-renewal of SSCs.**

236 (A) Expression of *Srsf1* in 5 dpp mouse testes. The RT–qPCR data were normalized to *Gapdh*. *n*=5. The expression

237 of *Srsf1* is shown as reading coverage in 5 dpp mouse testes.

238 (B) Western blotting of SRSF1 expression in 5 dpp mouse testes. ACTB served as a loading control. The value in

Ctrl testes was set as 1.0, and the relative values in cKO testes are indicated. n=5.

(C) Volcano map displaying the distribution of differentially expressed genes from RNA-seq data. The abscissa in the figure represents the gene fold change in 5 dpp cKO and Ctrl mouse testes. |log2FoldChange| ≥ 0. The ordinate indicates the significance of gene expression differences between 5 dpp cKO and Ctrl mouse testes. padj ≤ 0.05. Upregulated genes are shown as red dots, and downregulated genes are shown as green dots.

(D) Cluster heatmap of differentially expressed genes. The abscissa is the genotype, and the ordinate is the normalized FPKM (fragments per kilobase million) value of the differentially expressed gene. Red indicates a higher expression level, while green indicates a lower expression level.

(E) Network showing GO enrichment analyses of differentially expressed genes.

(F) Heatmap of spermatogonia-related gene expression.

(G) The expression of spermatogonia-related genes is shown as read coverage.

(H) The expression of spermatogonia-related genes in 5 dpp cKO and Ctrl mouse testes. The RT–qPCR data were normalized to *Gapdh*. The value in the Ctrl group was set as 1.0, and the relative value in the cKO group is indicated. n=3. Unpaired Student's t test determined significance; exact P value $P \geq 0.05$, $^{*}P < 0.05$, $^{**}P < 0.01$, $^{***}P < 0.001$, $^{****}P < 0.0001$. The points and error bars represent the mean ± SEM.

SRSF1 directly binds and regulates the expression and AS of *Tial1*/*Tiar*

Multiomics analyses were carried out in a subsequent study to identify the molecular mechanism of SRSF1 regulation that regulates the homing and self-renewal of SSCs. Venn diagram data revealed that 9 out of 715 down-regulated genes were bound by SRSF1 and underwent abnormal AS (Figure 7A). Furthermore, one out of 258 upregulated genes was bound by SRSF1 and underwent abnormal AS (Figure 7A). The AS genes were subsequently investigated in 5 dpp cKO mouse testes using transcriptomic analyses. RNA-seq analyses showed that 162 AS events were significantly affected (FDR<0.05) in cKO mouse testes (Figure 7B, 7C and Table S3). Most of the 133 affected AS events (162) were classified as skipped exons (SEs), with ten AS events categorized as retained introns (RIs), 13 as mutually exclusive exons (MXEs), four as alternative 5' splice sites (A5SSs), and two as alternative 3' splice sites (A3SSs) (Figure 7C). Additionally, the overall analysis of aberrant AS events showed that SRSF1 effectively promotes the occurrence of SE and MXE events and inhibits the occurrence of RI events. (Figure 7C). Then, GO enrichment analyses of AS genes revealed that four genes concerning germ cell development were altered in AS forms (Figure 7D). Thus, multiomics analyses suggested that *Tial1*/*Tiar* were posttranscriptionally regulated by SRSF1. RT–PCR results showed that the pre-mRNA of *Tial1*/*Tiar* in 5 dpp cKO mouse testes exhibited abnormal AS (Figure 7E). We then visualized the

different types of AS based on RNA-seq data by using IGV (Figure 7F). The results of RIP–qPCR showed that SRSF1 could bind to the pre-mRNA of *Tial1*/*Tiar* (Figure 7G). Interestingly, visual analysis using IGV showed that the peak of *Tial1*/*Tiar* was stabilized in 5 dpp cKO mouse testes (Figure 7H). RT–qPCR results showed that *Tial1*/*Tiar* transcript levels were not inhibited (Figure 7I). However, Western blotting showed that TIAL1/TIAR expression levels were significantly suppressed (Figure 7J). In summary, the data indicate that SRSF1 is required for TIAL1/TIAR expression and splicing in SSC homing and self-renewal.

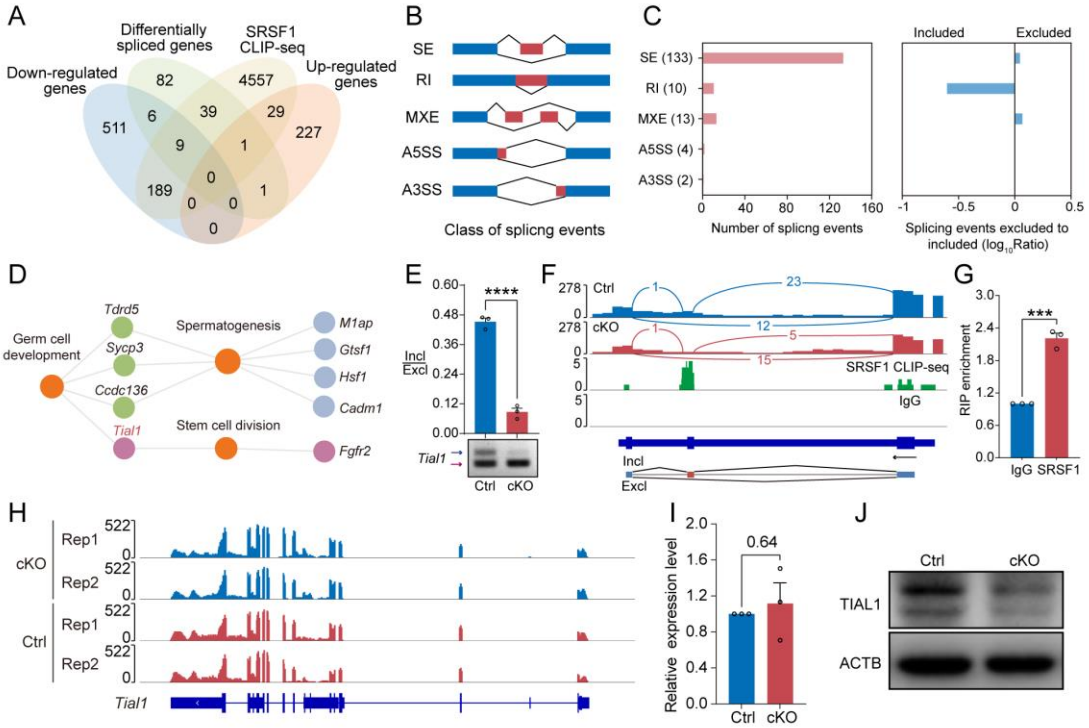

Figure 7 SRSF1 directly binds and regulates the expression and AS of *Tial1*/*Tiar*.

(A) Venn diagram showing the correlation among down-regulated, upregulated, alternatively spliced, and SRSF1-binding genes.

(B) Schematic diagram showing the classes of splicing events.

(C) Splicing events were analysed by number, exclusion, and inclusion.

(D) Network showing GO enrichment analyses of AS genes.

(E) The ectopic splicing of *Tial1/Tiar* in 5 dpp cKO and Ctrl mouse testes was analysed by RT–PCR. *n*=3. The ratio of inclusion (Incl) to exclusion (Excl) is shown accordingly.

(F) Analyses of *Tial1/Tiar* expression and exon–exon junctions were performed.

(G) SRSF1 directly regulated the expression of spermatogonia-related genes by RIP–qPCR in 5 dpp mouse testes. *n*=3.

(H) The expression of *Tial1*/*Tiar* is shown as read coverage.

(I) The expression of *Tial1*/*Tiar* in 5 dpp cKO and Ctrl mouse testes. The RT–qPCR data were normalized to *Gapdh*. The value in the Ctrl group was set as 1.0, and the relative value in the cKO group is indicated. n=3.

(J) Western blotting of TIAL1/TIAR expression in 5 dpp mouse testes. ACTB served as a loading control.

Unpaired Student's t test determined significance; exact P value $P \geq 0.05$, ***$P < 0.001$, ****$P < 0.0001$. The points and error bars represent the mean ± SEM.

SRSF1 recruits AS-related proteins to modulate AS in testes

To identify the interacting proteins for which SRSF1 exerts its AS role, we performed MS analyses of IP samples from 5 dpp mouse testis extracts. The silver-stained gel of SRSF1 and normal IgG showed several SRSF1-interacting proteins from 5 dpp mouse testis extracts (Figure 8A). The IP results indicated that SRSF1 was able to effectively IP the testis extracts of 5 dpp mice (Figure 8B). IP-MS data demonstrated the efficient enrichment of SRSF1 (Figure 8C and Table S4). These data showed that the two samples were highly reproducible, especially for SRSF1 (Figure 8D). Then, GO enrichment analyses of the IP proteins revealed that AS-related proteins could interact with SRSF1 (Figure 8E). A circular heatmap showed that SRSF1 could interact with AS-related proteins (e.g., SRSF10, SART1, RBM15, SRRM2, SF3B6, and SF3A2) (Figure 8F). Determining the complex structures of these interactions is valuable, in which molecular docking has played an important role (Yan et al., 2017). HDOCK is a novel web server of our hybrid docking algorithm of template-based modelling and free docking (Yan *et al.*, 2017). The HDOCK analysis results depicted SRSF1 with SRSF10, SART1, and RBM15 docking based on a hybrid strategy (Figure 8G). Together, the above data show that SRSF1 interacts with SRSF10, SART1, and RBM15 in 5 dpp mouse testes.

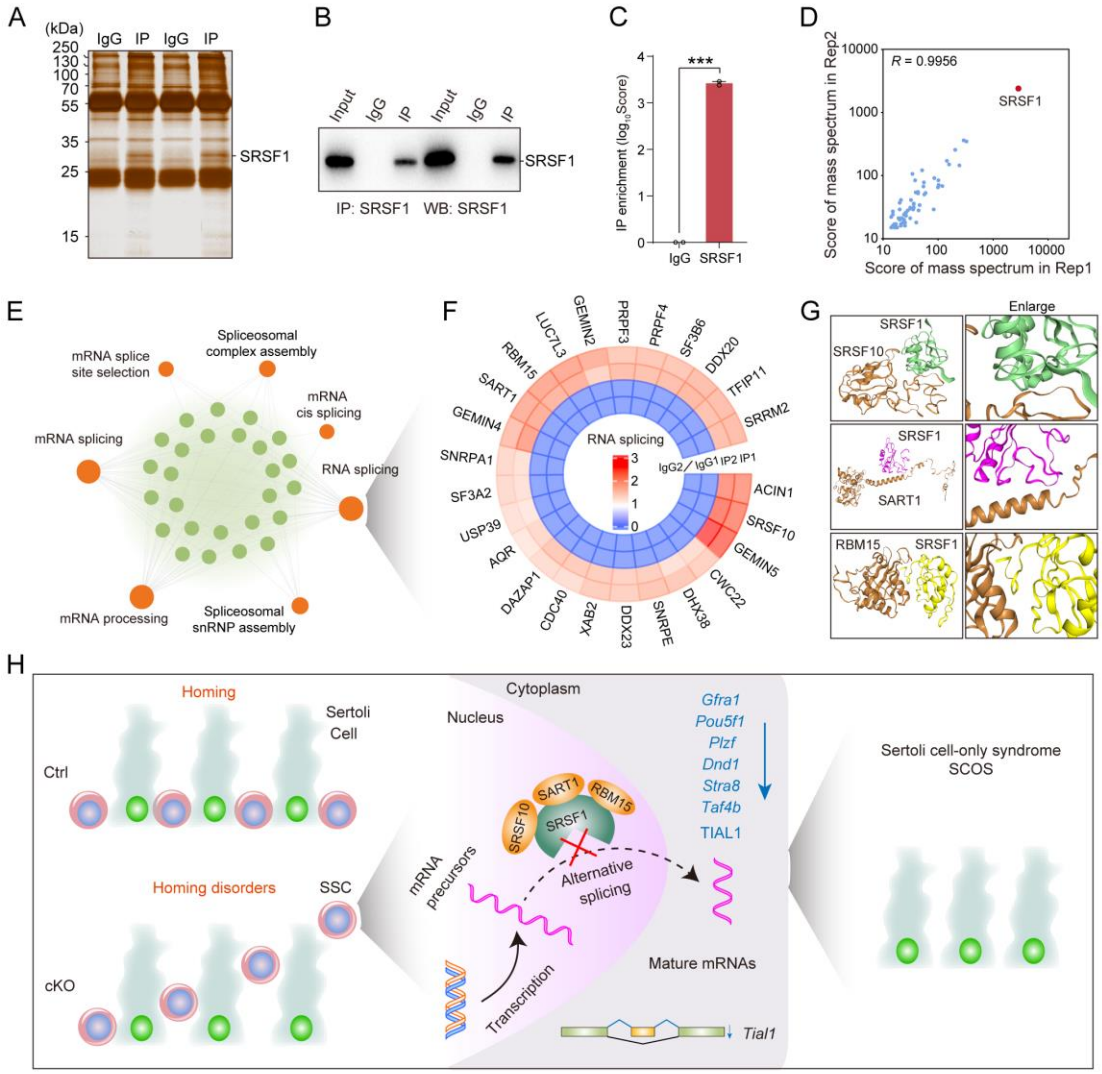

Figure 8 SRSF1 recruits AS-related proteins to modulate AS in testes.

(A) Silver-stained gel of SRSF1 and control immunoprecipitates from 5 dpp mouse testis extracts.

(B) IP experiment was performed in 5 dpp mouse testis extracts.

(C) IP of SRSF1 from IP-MS data.

(D) *Pearson's* correlation analysis showed the coefficient between the two samples for IP-MS data.

(E) Network showing GO enrichment analyses of SRSF1-binding proteins.

(F) Circular heatmap of AS-related proteins.

(G) A schematic diagram of protein interactions is shown.

(H) Schematic illustration of the molecular mechanisms by which SRSF1 regulates homing and self-renewal in mouse SSCs.

Discussion

Failure of spermatogonia survival led to SCOS

Disturbed spermatogenesis can cause SCOS and ultimately male sterility (Jiao et al., 2021). In recent years, it has been reported that many spermatogonia-related gene deletions have disrupted SSC self-renewal and differentiation in patient and mouse models (La and Hobbs, 2019a; Tan and Wilkinson, 2020; Wang et al., 2021). SCOS was observed in *Ddx5*, *Tial1*/*Tiar*, *Uhrf1*, *Pramef12*, *Dot1l*, and *Rad51* deletion mouse models (Beck et al., 1998; Legrand *et al.*, 2019; Lin et al., 2022; Qin et al., 2022; Wang et al., 2019; Zhou *et al.*, 2022). Mouse models are still of great significance and reference for human SCOS studies, and they will provide a better understanding of how SCOS occurs and develops over time. Interestingly, our mouse model had SCOS (Figure 3D-I and Figure 4). The absence of germ cells represents classical SCOS in adult mouse testes (Figure 4) (Wang *et al.*, 2023). In addition, we found abnormal expression of spermatogonia-related genes (*Gfra1*, *Pou5f1*, *Plzf*, *Dnd1*, *Stra8*, and *Taf4b*) in cKO mouse testes (Figure 6 F-H). These differentially expressed genes regulate SSC self-renewal and differentiation in mouse testes (Kanatsu-Shinohara and Shinohara, 2013; La and Hobbs, 2019a; Tan and Wilkinson, 2020). Thus, this provided an opportunity for us to better study the underlying molecular mechanisms. These data indicate that SRSF1 deficiency impairs spermatogonial survival, leading to SCOS in male mice.

The formation of SSC pools and the establishment of niches are essential for spermatogenesis

The earliest event in the development of the SSC population is the migration of prospermatogonia from the centre of seminiferous cords where they have resided since sex determination of the embryonic gonad to the basement membrane (Oatley and Brinster, 2012). In mice, this process is also known as homing, which occurs in the first 3 dpp and then develops into SSCs at 4 to 6 dpp for continuous self-renewal and differentiation (Lee and Shinohara, 2011; McLean *et al.*, 2003; Oatley and Brinster, 2012; Tan and Wilkinson, 2020). Therefore, homing analysis was performed in 5 dpp cKO mouse testes. Interestingly, the VASA and SOX9 co-staining results demonstrated that partial germ cells could not complete homing in 5 dpp cKO testes (Figure 5E). Germ cells that do not migrate to the basement membrane are unable to form SSC pools and establish niches (McLean *et al.*, 2003). These SSCs that lose their ecological niche will cease to exist. In our data, TUNEL results showed that apoptosis significantly increased in 7 dpp cKO mouse testes. At once, the germ cell count per tube showed a significant reduction in 7 dpp and 14 dpp cKO testes, especially 14 dpp cKO testes (Figure 5C). In conclusion, SRSF1 is crucial for the

formation of SSC pools and the establishment of niches through SSC homing.

Abnormal AS of *Tial1*/*Tiar* impaired the survival of spermatogonia

AS is commonly found in mammals, especially in the brain and testes (Mazin *et al.*, 2021; Merkin et al., 2012; Wang et al., 2008). AS plays essential roles in the posttranscriptional regulation of gene expression during many developmental processes, such as SSC self-renewal and differentiation (Chen et al., 2018; Song et al., 2020). Recently, BUD31-mediated AS of *Cdk2* was shown to be required for SSC self-renewal and differentiation (Qin *et al.*, 2023). *Srsf10* depletion disturbed the AS of genes, including *Nasp*, *Bclaf1*, *Rif1*, *Dazl*, *Kit*, *Ret*, and *Sycp1* (Liu *et al.*, 2022). UHRF1 interacts with snRNAs and regulates AS of *Tle3* in mouse SSCs (Zhou *et al.*, 2022). Mettl3-mediated m6A regulates AS of *Sohlh1* and *Dazl* (Xu et al., 2017). We found that SRSF1 acts as an alternative RNA splicing regulator and directly interacts with *Tial1*/*Tiar* transcripts to regulate splicing events in spermatogonia (Figure 7E-G). Additionally, TIAL1/TIAR expression levels were significantly suppressed (Figure 7J). Interestingly, *Tial1*/*Tiar* transcript levels were not inhibited (Figure 7H and 7I). These results suggested that SRSF1 explicitly regulates the expression of *Tial1*/*Tiar* via AS. Studies have reported that TIAL1/TIAR is essential for primordial germ cell development in mouse testes (Beck *et al.*, 1998). *Tial1/Tiar* deletion impairs spermatogonia survival leading to SCOS, consistent with our phenotype (Figure 3E-I and 4A-C) (Beck *et al.*, 1998). To summarize, SRSF1 directly binds and regulates the expression of *Tial1*/*Tiar* via AS to implement SSC homing and self-renewal.

We found that SRSF1 could interact with AS-related proteins (e.g., SRSF10, SART1, RBM15, SRRM2, SF3B6, and SF3A2) (Figure 8F). A recent study reported that SRSF10 deficiency impaired spermatogonia differentiation but did not affect spermatogonia homing and self-renewal (Liu *et al.*, 2022). However, our data showed that SRSF1 is essential for homing and self-renewal in mouse SSCs. Therefore, this suggests that SRSF1 has a specific function in the homing and self-renewal of SSCs that are not bound by SRSF10.

SRSF1-mediated posttranscriptional regulation during SSC homing and self-renewal provides new insights into the treatment of human reproductive diseases

Aberrant SSC homing and self-renewal often lead to gametogenic failure or produce aneuploid gametes, resulting in subfertility or infertility, miscarriage, or congenital disabilities (Jiao *et al.*, 2021; Kanatsu-Shinohara and Shinohara, 2013; La and Hobbs, 2019a; Song and Wilkinson, 2014). Loss-of-function mutations in humans and corresponding knockout/mutated mice have been extensively researched (Jiao

386 *et al.*, 2021). However, AS-related posttranscriptional regulation during meiosis has not been well
387 studied. In recent years, there have been reports that the RNA-binding proteins SRSF10, UHRF1, BUD31,
388 and BCAS2 regulate AS in mouse SSCs (Liu *et al.*, 2022; Liu *et al.*, 2017; Qin *et al.*, 2023; Zhou *et al.*,
389 2022). This study used a multiomics approach to perform in-depth analyses of SRSF1-mediated
390 posttranscriptional regulatory mechanisms to enrich the field. It also provides new ideas and insights for
391 clinical diagnosis and treatment.
392 In summary, this study demonstrates that SRSF1 plays a critical role in posttranscriptional regulation by
393 explicitly regulating the expression of *Tial1*/*Tiar* via AS to implement SSC homing and self-renewal
394 (Figure 8H). Thus, the posttranscriptional regulation of SRSF1-mediated splicing is resolved during the
395 formation of SSC pools and the establishment of niches.
396
397 **Materials and Methods**
398 **Mouse strains**
399 C57BL/6N and ICR mice were purchased from Beijing Vital River Laboratory Animal Technology Co.,
400 Ltd. *Srsf1*$^{Fl/Fl}$ mice were generated in the laboratory of Prof. Xiangdong Fu (University of California, San
401 Diego, USA) and were kindly provided by Prof. Yuanchao Xue (Institute of Biophysics, Chinese
402 Academy of Sciences, Beijing, China) (Xu *et al.*, 2005). *Vasa*-Cre mice were obtained from The Jackson
403 Laboratory (Gallardo et al., 2007).To generate *Srsf1* cKO mice, *Vasa*-Cre mice were crossed with
404 *Srsf1*$^{Fl/Fl}$ mice. The primers used for PCR to genotype *Srsf1*$^{Fl/Fl}$ and *Vasa*-Cre mice are shown in Table
405 S5. All mice were bred and housed under specific pathogen-free conditions with a controlled temperature
406 (22 ± 1°C) and exposed to a constant 12-hour light-dark cycle in the animal facilities of China
407 Agricultural University. All experiments were conducted according to the guidelines and with the
408 approval of the Institutional Animal Care and Use Committee of China Agricultural University (No.
409 AW80401202-3-3).
410 **Fertility test**
411 For 15 days, two 8-week-old ICR female mice were caged with one 8-week-old male control (Ctrl) or
412 cKO mouse. The mice were kept individually after the appearance of the vaginal plug, and the dates were
413 recorded. Male mice continue to be caged after two days. The number of pups from each female was
414 recorded each day, and the date of parturition was recorded.
415 **Immunostaining and histological analyses**

Mouse testes were fixed with 4% paraformaldehyde (PFA, P6148-500G, Sigma–Aldrich) in PBS (pH 7.4) at 4°C overnight, dehydrated in graded ethanol solutions, vitrified with xylene, and embedded in paraffin. Testis sections were cut at a 5-μm thickness for immunostaining and histologic analyses. For histological analyses, sections were dewaxed in xylene, rehydrated in a graded ethanol solution, and stained with haematoxylin. After sealing the slides with neutral resin, a Ventana DP200 system was used for imaging. For immunofluorescence analyses, antigen retrieval was performed by microwaving the sections with sodium citrate buffer (pH 6.0). After blocking with 10% normal goat serum at room temperature for 1 hour, the sections were incubated with primary antibodies (Table S6) in 5% normal goat serum overnight at 4°C. After washing with PBS, the sections were incubated with secondary antibodies (Table S6) at room temperature in the dark for 1 hour. The slides were mounted in an antifade mounting medium with DAPI (P0131, Beyotime). Photographs were taken with a Nikon A1 laser scanning confocal microscope and a Zeiss OPTOME fluorescence microscope.

Whole-mount immunostaining

The testes were collected and dispersed with 5ml syringes. Blown-out tubules were fixed in PFA at 4°C for 4 hours. The tubules were washed three times with PBS (pH 7.4) for 5 min each and stored at 4°C. The tubules were permeated with 0.3% Triton X-100 for 1 h at 4°C. Then, whole-mount staining followed the immunostaining protocol.

TUNEL apoptosis analyses

7 dpp testis sections were prepared as described in the instructions for the TUNEL Apoptosis Assay Kit (C1088, Beyotime). Photographs were taken with a Nikon A1 laser scanning confocal microscope and a Zeiss OPTOME fluorescence microscope.

RT–PCR and RT–qPCR

Total RNA was extracted by using RNAiso Plus (9109, Takara), and the concentration was measured with a Nano-300 ultramicro spectrophotometer (Allsheng). cDNA was obtained according to the instructions of a TIANScript II RT kit (KR107, TIANGEN). The expression of transcripts of the target gene was measured by using a LightCycle® 96 instrument (Roche) with Hieff UNICON SYBR green master mix (11198ES08, Yeasen). AS analyses were performed on a RePure-A PCR instrument (BIO-GENER). Primers were synthesized by Sangon Biotech (Table S5). The expression level of *Gapdh* or *Actb* was used as the control, and this value was set as 1. Other samples' relative transcript expression levels were obtained by comparing them with the control results.

RNA-seq

Total RNA was extracted from mouse testes according to the above protocol at 5 dpp. Briefly, mRNA was purified from total RNA using poly-T oligo-attached magnetic beads. After fragmentation, we established a transcriptome sequencing library and assessed library quality on an Agilent Bioanalyzer 2100 system. The clustering of the index-coded samples was performed on a cBot Cluster Generation System using a TruSeq PE Cluster kit v3-cBot-HS (Illumina) according to the manufacturer's instructions. After cluster generation, the library preparations were sequenced on the Illumina NovaSeq platform, and 150 bp paired-end reads were generated. After quality control, all downstream analyses were performed on clean, high-quality data. The reference genome index was built, and paired-end clean reads were aligned to the reference genome using HISAT2 software (version 2.0.5). FeatureCounts (version 1.5.0) counted the reads mapped to each gene. Then, the fragments per kilobase million (FPKM) value of each gene was calculated based on the length of the gene and the read count mapped to this gene. Differential expression analyses of cKO/Ctrl mouse testes (three biological replicates per condition) were performed using the DESeq2 R package (version 1.20.0). Genes with a padj $\leq$ 0.05 identified by DESeq2 were considered differentially expressed.

AS analyses

rMATS software (version 3.2.5) was used to analyse the AS events in cKO mouse germ cells based on RNA-seq data. Five types of AS events (SE, RI, MXE, A5SS, and A3SS) were revealed by rMATS software. Our threshold for screening differentially significant AS events was a false discovery rate (FDR) of less than 0.05. Splicing events with an FDR less than 0.05 and an inclusion-level difference with a significance of at least 5% (0.05) were considered statistically significant. Integrative Genomics Viewer (IGV, 2.16.0) software was used to visualize and confirm AS events based on RNA-seq data.

Gene Ontology (GO) enrichment analyses

The GO enrichment analyses of differentially expressed genes and AS genes were implemented with the clusterProfiler R package (version 3.4.4), in which gene length bias was corrected. GRCm38/mm10 was used as a mouse reference genome, and the Benjamini–Hochberg multiple methods was applied to adjust for multiple testing. GO enrichment analyses with corrected *P* values of less than 0.05 were significantly enriched for differentially expressed genes and AS genes.

Western blotting

Total protein was extracted with cell lysis buffer (P0013, Beyotime) containing PMSF (1:100, ST506, Beyotime) and a protease inhibitor cocktail (1:100, P1005, Beyotime). A BCA protein assay kit (CW0014S, CWBiotech) measured the protein concentration. The protein lysates were electrophoretically separated on sodium dodecyl sulfate-polyacrylamide gels and electrically transferred to polyvinylidene fluoride membranes (IPVH00010, Millipore). The membranes were blocked in 5% skimmed milk for 1 hour and incubated with the primary antibodies (Table S6) for one night at 4°C. Then, the membranes were incubated with secondary antibodies (Table S6) at room temperature for 1 hour. The proteins were visualized using a Tanon 5200 chemiluminescence imaging system following incubation with BeyoECL Plus (P0018S, Beyotime).

IP, IP-MS, Co-IP

Total protein was extracted with cell lysis buffer (P0013, Beyotime) containing PMSF (1:100, ST506, Beyotime) and a protease inhibitor cocktail (1:100, P1005, Beyotime). After incubation on ice for 20 min, the lysate was added to 20 μl of protein A agarose (P2051-2 ml, Beyotime) for pre-clearing at 4°C for 1 hour. Two micrograms of an SRSF1 antibody (sc-33652, Santa Cruz Biotechnology) and a normal mouse IgG (sc-3879, Santa Cruz Biotechnology) were added to the lysate the mixture was incubated overnight incubation at 4°C. The next day, 60 μl of protein A agarose was added to the lysate, which was then incubated at 4°C for 4 hours. The agarose complexes containing antibodies and target proteins were washed 3 times for 5 min at 4°C. IP and Co-IP were performed according to the above Western blotting protocol. The complex was sent to the protein mass spectrometry laboratory for IP-MS analyses using a Thermo Q-Exactive high-resolution mass spectrometer (Thermo Scientific, Waltham). Raw data from the mass spectrometer were preprocessed with Mascot Distiller 2.4 for peak picking. The resulting peak lists were searched against the uniport mouse database using Mascot 2.5 search engine.

RNA immunoprecipitation (RIP) and RIP–qPCR

As described previously (Gagliardi and Matarazzo, 2016), RIP was performed using 5 dpp mouse testes. The testes were lysed in cell lysis buffer (P0013, Beyotime) containing PMSF (1:100, ST506, Beyotime), a proteinase inhibitor cocktail (1:100, P1005, Beyotime), DTT (1:50, ST041-2 ml, Beyotime), and an RNase inhibitor (1:20, R0102-10 kU, Beyotime). After incubation on ice for 20 min, the lysate was added to 20 μl of protein A agarose (P2051-2 ml, Beyotime) for pre-clearing at 4°C for 1 hour. Two micrograms of an SRSF1 antibody (sc-33652, Santa Cruz Biotechnology) and a normal mouse IgG (sc-3879, Santa Cruz Biotechnology) were added to the lysate, which was then incubated overnight at 4°C. The next day,

60 μl of protein A agarose was added to the lysate, and the mixture was incubated at 4°C for 4 hours. The agarose complexes containing antibodies, target proteins, and RNA were washed 3 times for 5 min at 4°C and repeated. Protein-bound RNA was extracted using RNAiso Plus and a Direct-zol RNA MicroPrep Kit. RIP–qPCR was performed according to the above RT–qPCR protocol.

CLIP-seq library construction and data analysis

Total cells were isolated from adult WT C57BL/6N mouse testes, and then the cells were crosslinked by ultraviolet light (254 nm) to maintain the covalent binding of RBPs to their cognate RNA. Subsequently, SRSF1 and crosslinked RNAs were immunoprecipitated with an anti-SRSF1 antibody and digested with micrococcal nuclease (EN0181, Thermo Fisher Scientific). An IR800-biotin adapter was ligated to the 3′ ends of the RNA fragments. Then, the SRSF1/RNA complexes were separated by SDS–PAGE and transferred to a nitrocellulose membrane (HATF00010, Millipore). These RNA and protein complexes from approximately 47 to 62 kDa were extracted from the nitrocellulose membrane, after which proteinase K (9034, Takara) digestion was performed. RNA was isolated with saturated phenol (AM9712, Ambion), ligated with adaptors, and converted to cDNA with a SuperScript III First-Strand Kit (18080-051, Invitrogen). The cDNA was amplified by PCR to prepare the corresponding libraries and then sequenced on illumina NovaSeq 6000.

For the analyses of CLIP-seq data, the adaptor sequences were first removed from the reads by Trimmomatic (version 0.36). Subsequently, Bowtie 2 (version 2.1.0) was applied for mapping of clean reads to the mm10 reference genome with the parameters "-p 10 -L 15 -N 1 -D 50 -R 50 --phred33 --qc-filter --very-sensitive --end-to-end." CLIP-seq peaks were identified by Piranha (version 1.2.1) with the following parameters: "-s -b 20 -d Zero Truncated Negative Binomial -p 0.05."

Statistical analyses

Pearson's correlation coefficients (R) were calculated by using the scores of the two samples for MS or the reads of two SRSF1 CLIP-seq libraries. The Kolmogorov–Smirnov test was used to compare the distributions of CLIP-seq signals for two sets of genes. GraphPad Prism software (version 9.0.0) was used for the statistical analyses, and the values and error bars represent the mean ± SEM. Significant differences between the two groups were analysed using Student's *t* test. Statistical significance is indicated as follows: exact *P* value $P \geq 0.05$; *$P < 0.05$; **$P < 0.01$; ***$P < 0.001$; ****$P < 0.0001$).

Acknowledgments

This work was supported by the National Natural Science Foundation of China (32171111); and the Beijing Natural Science Foundation (5222015). We thank Prof. Yuanchao Xue (Institute of Biophysics, Chinese Academy of Sciences, Beijing, China) for sharing *Srsf1*$^{Fl/Fl}$ mice, Prof. Shuyang Yu, Hua Zhang and Chao Wang (China Agricultural University, Beijing, China) for thoughtful discussions and suggestions, and all the members of Prof. Hua Zhang, Chao Wang, and Shuyang Yu laboratory for helpful discussions and comments. We thank Novogene for their assistance with the RNA-seq and CLIP-seq experiments.

References

Beck, A.R., Miller, I.J., Anderson, P., and Streuli, M. (1998). RNA-binding protein TIAR is essential for primordial germ cell development. Proc Natl Acad Sci U S A *95*, 2331-2336. 10.1073/pnas.95.5.2331.

Cafe, S.L., Skerrett-Byrne, D.A., De Oliveira, C.S., Nixon, B., Oatley, M.J., Oatley, J.M., and Lord, T. (2021). A regulatory role for CHD4 in maintenance of the spermatogonial stem cell pool. Stem cell reports *16*, 1555-1567. 10.1016/j.stemcr.2021.04.003.

Chen, Y., Zheng, Y., Gao, Y., Lin, Z., Yang, S., Wang, T., Wang, Q., Xie, N., Hua, R., Liu, M., et al. (2018). Single-cell RNA-seq uncovers dynamic processes and critical regulators in mouse spermatogenesis. Cell Res *28*, 879-896. 10.1038/s41422-018-0074-y.

Du, J.X., Luo, Y.H., Zhang, S.J., Wang, B., Chen, C., Zhu, G.Q., Zhu, P., Cai, C.Z., Wan, J.L., Cai, J.L., et al. (2021). Splicing factor SRSF1 promotes breast cancer progression via oncogenic splice switching of PTPMT1. J Exp Clin Cancer Res *40*, 171. 10.1186/s13046-021-01978-8.

Gagliardi, M., and Matarazzo, M.R. (2016). RIP: RNA Immunoprecipitation. Methods Mol Biol *1480*, 73-86. 10.1007/978-1-4939-6380-5_7.

Gallardo, T., Shirley, L., John, G.B., and Castrillon, D.H. (2007). Generation of a germ cell-specific mouse transgenic Cre line, Vasa-Cre. Genesis (New York, N.Y. : 2000) *45*, 413-417. 10.1002/dvg.20310.

Jiao, S.Y., Yang, Y.H., and Chen, S.R. (2021). Molecular genetics of infertility: loss-of-function mutations in humans and corresponding knockout/mutated mice. Hum Reprod Update *27*, 154-189. 10.1093/humupd/dmaa034.

Juul, A., Almstrup, K., Andersson, A.M., Jensen, T.K., Jorgensen, N., Main, K.M., Rajpert-De Meyts, E., Toppari, J., and Skakkebaek, N.E. (2014). Possible fetal determinants of male infertility. Nature reviews. Endocrinology *10*, 553-562. 10.1038/nrendo.2014.97.

Kanatsu-Shinohara, M., and Shinohara, T. (2013). Spermatogonial stem cell self-renewal and development. Annual review of cell and developmental biology *29*, 163-187. 10.1146/annurev-cellbio-101512-122353.

Katsuyama, T., Li, H., Comte, D., Tsokos, G.C., and Moulton, V.R. (2019). Splicing factor SRSF1 controls T cell hyperactivity and systemic autoimmunity. J Clin Invest *129*, 5411-5423. 10.1172/JCI127949.

Katsuyama, T., and Moulton, V.R. (2021). Splicing factor SRSF1 is indispensable for regulatory T cell homeostasis and function. Cell Rep *36*, 109339. 10.1016/j.celrep.2021.109339.

Kluin, P.M., and de Rooij, D.G. (1981). A comparison between the morphology and cell kinetics of gonocytes and adult type undifferentiated spermatogonia in the mouse. International journal of andrology *4*, 475-493. 10.1111/j.1365-2605.1981.tb00732.x.

La, H.M., and Hobbs, R.M. (2019a). Mechanisms regulating mammalian spermatogenesis and fertility recovery following germ cell depletion. Cell Mol Life Sci *76*, 4071-4102. 10.1007/s00018-019-03201-6.

La, H.M., and Hobbs, R.M. (2019b). Mechanisms regulating mammalian spermatogenesis and fertility recovery following germ cell depletion. Cell Mol Life Sci *76*, 4071-4102. 10.1007/s00018-019-03201-6.

Law, N.C., Oatley, M.J., and Oatley, J.M. (2019). Developmental kinetics and transcriptome dynamics of stem cell specification in the spermatogenic lineage. Nat Commun *10*, 2787. 10.1038/s41467-019-10596-0.

Lee, J., and Shinohara, T. (2011). Epigenetic modifications and self-renewal regulation of mouse germline stem cells. Cell Res *21*, 1164-1171. 10.1038/cr.2011.111.

Legrand, J.M.D., Chan, A.L., La, H.M., Rossello, F.J., Anko, M.L., Fuller-Pace, F.V., and Hobbs, R.M. (2019). DDX5 plays essential transcriptional and post-transcriptional roles in the maintenance and function of spermatogonia. Nat Commun *10*, 2278. 10.1038/s41467-019-09972-7.

Lin, H., Cheng, K., Kubota, H., Lan, Y., Riedel, S.S., Kakiuchi, K., Sasaki, K., Bernt, K.M., Bartolomei, M.S., Luo, M., and Wang, P.J. (2022). Histone methyltransferase DOT1L is essential for self-renewal of germline stem cells. Genes Dev *36*, 752-763. 10.1101/gad.349550.122.

Liu, J., You, M., Yao, Y., Ji, C., Wang, Z., Wang, F., Wang, D., Qi, Z., Yu, G., Sun, Z., et al. (2021). SRSF1 plays a critical role in invariant natural killer T cell development and function. Cell Mol Immunol *18*, 2502-2515. 10.1038/s41423-021-00766-w.

Liu, W., Lu, X., Zhao, Z.H., Su, R., Li, Q.L., Xue, Y., Gao, Z., Sun, S.S., Lei, W.L., Li, L., et al. (2022). SRSF10 is essential for progenitor spermatogonia expansion by regulating alternative splicing. eLife *11*. 10.7554/eLife.78211.

Liu, W., Wang, F., Xu, Q., Shi, J., Zhang, X., Lu, X., Zhao, Z.A., Gao, Z., Ma, H., Duan, E., et al. (2017). BCAS2 is involved in alternative mRNA splicing in spermatogonia and the transition to meiosis. Nat Commun *8*, 14182. 10.1038/ncomms14182.

Lv, Y., Zhang, W., Zhao, J., Sun, B., Qi, Y., Ji, H., Chen, C., Zhang, J., Sheng, J., Wang, T., et al. (2021). SRSF1 inhibits autophagy through regulating Bcl-x splicing and interacting with PIK3C3 in lung cancer. Signal Transduct Target Ther *6*, 108. 10.1038/s41392-021-00495-6.

Mazin, P.V., Khaitovich, P., Cardoso-Moreira, M., and Kaessmann, H. (2021). Alternative splicing during mammalian organ development. Nat Genet *53*, 925-934. 10.1038/s41588-021-00851-w.

McLean, D.J., Friel, P.J., Johnston, D.S., and Griswold, M.D. (2003). Characterization of spermatogonial stem cell maturation and differentiation in neonatal mice. Biol Reprod *69*, 2085-2091. 10.1095/biolreprod.103.017020.

Merkin, J., Russell, C., Chen, P., and Burge, C.B. (2012). Evolutionary dynamics of gene and isoform regulation in Mammalian tissues. Science *338*, 1593-1599. 10.1126/science.1228186.

Oatley, J.M., and Brinster, R.L. (2012). The germline stem cell niche unit in mammalian testes. Physiological reviews *92*, 577-595. 10.1152/physrev.00025.2011.

Qi, Z., Wang, F., Yu, G., Wang, D., Yao, Y., You, M., Liu, J., Liu, J., Sun, Z., Ji, C., et al. (2021). SRSF1 serves as a critical posttranscriptional regulator at the late stage of thymocyte development. Sci Adv *7*. 10.1126/sciadv.abf0753.

Qin, J., Huang, T., Wang, J., Xu, L., Dang, Q., Xu, X., Liu, H., Liu, Z., Shao, C., and Zhang, X. (2022). RAD51 is essential for spermatogenesis and male fertility in mice. Cell death discovery *8*, 118. 10.1038/s41420-022-00921-w.

Qin, J., Huang, T., Wang, Z., Zhang, X., Wang, J., Dang, Q., Cui, D., Wang, X., Zhai, Y., Zhao, L., et al. (2023). Bud31-mediated alternative splicing is required for spermatogonial stem cell self-renewal and differentiation. Cell Death Differ *30*, 184-194. 10.1038/s41418-022-01057-1.

628 Song, H., Wang, L., Chen, D., and Li, F. (2020). The Function of Pre-mRNA Alternative Splicing
629 in Mammal Spermatogenesis. Int J Biol Sci *16*, 38-48. 10.7150/ijbs.34422.
630 Song, H.W., and Wilkinson, M.F. (2014). Transcriptional control of spermatogonial
631 maintenance and differentiation. Seminars in cell & developmental biology *30*, 14-26.
632 10.1016/j.semcdb.2014.02.005.
633 Sun, L., Lv, Z., Chen, X., Wang, C., Lv, P., Yan, L., Tian, S., Xie, X., Yao, X., Liu, J., et al. (2023).
634 SRSF1 regulates primordial follicle formation and number determination during meiotic
635 prophase I. BMC Biology *21*, 49. 10.1186/s12915-023-01549-7.
636 Tan, K., and Wilkinson, M.F. (2020). A single-cell view of spermatogonial stem cells. Current
637 opinion in cell biology *67*, 71-78. 10.1016/j.ceb.2020.07.005.
638 Venables, J.P. (2002). Alternative splicing in the testes. Current opinion in genetics &
639 development *12*, 615-619. 10.1016/s0959-437x(02)00347-7.
640 Wang, E.T., Sandberg, R., Luo, S., Khrebtukova, I., Zhang, L., Mayr, C., Kingsmore, S.F., Schroth,
641 G.P., and Burge, C.B. (2008). Alternative isoform regulation in human tissue transcriptomes.
642 Nature *456*, 470-476. 10.1038/nature07509.
643 Wang, X., Liu, X., Qu, M., and Li, H. (2023). Sertoli cell-only syndrome: advances, challenges,
644 and perspectives in genetics and mechanisms. Cell Mol Life Sci *80*, 67. 10.1007/s00018-023-
645 04723-w.
646 Wang, Y.H., Yan, M., Zhang, X., Liu, X.Y., Ding, Y.F., Lai, C.P., Tong, M.H., and Li, J.S. (2021).
647 Rescue of male infertility through correcting a genetic mutation causing meiotic arrest in
648 spermatogonial stem cells. Asian J Androl *23*, 590-599. 10.4103/aja.aja_97_20.
649 Wang, Z., Xu, X., Li, J.L., Palmer, C., Maric, D., and Dean, J. (2019). Sertoli cell-only phenotype
650 and scRNA-seq define PRAMEF12 as a factor essential for spermatogenesis in mice. Nat
651 Commun *10*, 5196. 10.1038/s41467-019-13193-3.
652 Xu, K., Yang, Y., Feng, G.H., Sun, B.F., Chen, J.Q., Li, Y.F., Chen, Y.S., Zhang, X.X., Wang, C.X.,
653 Jiang, L.Y., et al. (2017). Mettl3-mediated m(6)A regulates spermatogonial differentiation and
654 meiosis initiation. Cell Res *27*, 1100-1114. 10.1038/cr.2017.100.
655 Xu, X., Yang, D., Ding, J.H., Wang, W., Chu, P.H., Dalton, N.D., Wang, H.Y., Bermingham, J.R.,
656 Jr., Ye, Z., Liu, F., et al. (2005). ASF/SF2-regulated CaMKIIdelta alternative splicing temporally
657 reprograms excitation-contraction coupling in cardiac muscle. Cell *120*, 59-72.
658 10.1016/j.cell.2004.11.036.
659 Yamaji, M., Jishage, M., Meyer, C., Suryawanshi, H., Der, E., Yamaji, M., Garzia, A., Morozov,
660 P., Manickavel, S., McFarland, H.L., et al. (2017). DND1 maintains germline stem cells via
661 recruitment of the CCR4-NOT complex to target mRNAs. Nature *543*, 568-572.
662 10.1038/nature21690.
663 Yan, Y., Zhang, D., Zhou, P., Li, B., and Huang, S.Y. (2017). HDOCK: a web server for protein-
664 protein and protein-DNA/RNA docking based on a hybrid strategy. Nucleic Acids Res *45*,
665 W365-w373. 10.1093/nar/gkx407.
666 Zhou, S., Dong, J., Xiong, M., Gan, S., Wen, Y., Zhang, J., Wang, X., Yuan, S., and Gui, Y. (2022).
667 UHRF1 interacts with snRNAs and regulates alternative splicing in mouse spermatogonial stem
668 cells. Stem cell reports *17*, 1859-1873. 10.1016/j.stemcr.2022.06.010.

669